Regulation of Facilitative Glucose Transporters and AKT/MAPK/PRKAA Signaling via Estradiol and Progesterone in the Mouse Uterine Epithelium[1]

Sung Tae Kim and Kelle H. Moley[2]

Department of Obstetrics and Gynecology, Washington University School of Medicine, St. Louis, Missouri

ABSTRACT

Adequate uterine glucose metabolism is an essential part of embryo implantation and the development of an adequate utero-fetal environment. However, expression of facilitative glucose transporters (GLUTs [solute transporter family SLC2A]) and AKT/MAPK/PRKAA (PRKAA) signaling has not been described in the mouse uterine cells, to our knowledge. The objective of this study was to determine the hormonal regulation of SLC2A protein expression and AKT/MAPK/PRKAA signaling in the mouse uterine epithelial cells during estrous cycles and peri-implantation periods. SLC2As 1, 4, 8, and 9B were highly expressed in the luminal and glandular epithelia of estrous stage. In metestrous and diestrous stages, expression of SLC2As 1, 4, 8, and 9B was lower than that in proestrous stage. Levels of activated phospho-AKT (p-AKT), p-MAPK3, and p-MAPK1 also varied during the estrous cycle. Estrogen and progesterone injection in an ovariectomized mouse (delayed implantation model) resulted in a decrease and an increase, respectively, in expression of GLUTs in the luminal epithelial cells of the uterus. The expression of SLC2A1, SLC2A8, SLC2A9B, p-AKT, p-MAPK3/1, and p-PRKAA was increased in the decidual region of the implantation sites and was significantly increased in the uterus of activated implantation. Using an artificial decidualiza-tion mouse model, it was also demonstrated that expression of the same GLUTs, p-MAPK3/1, and p-PRKAA was dramatically higher in the decidualized uteri than that in the control uteri. These results suggest that steroid hormones regulate expression of uterine epithelial GLUTs possibly through AKT/MAPK/PRKAA signaling pathways and that glucose utilization may have an important role in decidualization and possibly in the mainte-nance of pregnancy.

epithelium, estradiol, female reproductive tract, implantation, progesterone, uterine epithelium, uterus

INTRODUCTION

The entry of glucose into the cells is facilitated by a family of glucose transporters (GLUTs) that are characterized by the presence of 12 membrane-spanning helices and several conserved sequence motifs. Thirteen members of the GLUT (SLC2A) family have been subdivided into three classes: class I consists of SLC2As 1, 2, 3, and 4; class II consists of SLC2As 5, 7, 9, and 11; and class III consists of SLC2As 6, 8, 10, and 12 and the H^+-coupled myoinositol transporter [1–3]. GLUTs exhibit a high degree of sequence homology; however, they differ in their substrate specificity, kinetic characteristics, tissue and subcellular distribution, and response to extracellular stimuli [1, 4].

SLC2A1 is associated with the basal uptake and storage of glucose in most cells [5]. SLC2A4 is well known as the important insulin-sensitive transporter and is expressed in insulin-responsive tissues [6, 7]. SLC2A8 is a recently cloned member of the class III facilitative transporters and is expressed in the heart, skeletal muscle, brain, spleen, prostate, intestine, and testis and in the developing embryo at blastocyst stage [8–11]. We have shown that SLC2A8 is an insulin-sensitive transporter in mouse blastocyst and testis [8, 12]. Also, we have identified and cloned mouse SLC2A9 [13]. A unique feature of mouse SLC2A9 is the existence of multiple splice variants, namely, mouse SLC2A9A (a long form having 12 transmembrane segments) and mouse SLC2A9B (two short forms each having a deletion resulting in the loss of two transmembrane-spanning domains) [14]. We have shown that SLC2A9A and SLC2A9B are differently expressed in the mouse sperm, testis, kidney, liver, and heart [9, 14]. Mouse SLC2A12 is cloned from preimplantation embryo and is expressed in heart, muscle, uterus, and fat [15].

AKT is a major component of the PI3-kinase signaling pathway and is known to participate in multiple physiological processes. In response to insulin, AKT controls the glucose uptake process by regulating insulin-mediated SLC2A4 translocation [16, 17]. A recent study [18] shows that prolactin induces MAPK1 phosphorylation in the glandular epithelium and the CD56$^+$ natural killer cells within the stromal compartment of the human endometrium. Another study [19] shows that uterine AKT and MAPK are activated by insulin-like growth factor (IGF) 1 and estrogen in mouse. AMP-activated protein kinase (PRKAA or PRKAA) is activated by an increase in the AMP:ATP ratio [20]. PRKAA has a key role in energy metabolism (e.g., fatty acid oxidation and synthesis, glucose uptake, and cholesterol synthesis [21, 22]). In addition, SLC2A4 translocation is mediated by PRKAA signaling in heart [23, 24]. However, GLUTs expression and AKT/MAPK/PRKAA signaling have not been explored (to our knowledge) in the mouse uterus in response to steroid hormones during estrous cycles and peri-implantation periods. The objective of this study was to investigate the expression and hormonal regulation of GLUTs and AKT/MAPK/PRKAA signaling in the uterus during estrous cycles and peri-implantation periods. Our rationale is that if we can further dissect the downstream metabolic pathways regulated by estradiol, progesterone, and pregnancy-related hormonal changes, then possibly nonhor-monal metabolic therapies can be applied to conditions of implantation failure and pregnancy loss.

MATERIALS AND METHODS

Animals and Tissue Preparation

Mice were housed according to institutional animal care and use committee and National Institutes of Health (Bethesda, MD) guidelines. Adult C57BL6 female mice purchased from the National Cancer Institute (Bethesda, MD) were mated with fertile male mice of the same strain to induce pregnancy (Day 1 [vaginal plug]). On Day 5 and Day 6 of pregnancy, implantation sites (IS) were visualized by an intravenous injection of Chicago blue dye solution (Sigma, St. Louis, MO). On Day 7 and Day 8, IS are distinct, and their identification does not require special manipulation. IS and inter-IS were immediately frozen in cold Friendly Freeze'it (Curtin Matheson Scientific, Houston, TX) and were stored at −75°C until protein extraction or cryosection. All experiments were conducted three times.

Western Blot Analysis

Western blot analysis was performed as described previously [9]. Briefly, total protein extract (~15 μg) was separated in a 10% SDS-polyacrylamide gel and was then transferred onto nitrocellulose membranes. Different gels were run for each experiment, and each individual gel was normalized to β-actin. After blocking with 5% nonfat dry milk powder in 1× Tris-buffered saline (TBS) and 0.05% Tween 20 (TBS-T) for 1 h at room temperature, the membranes were incubated with primary antibody (0.25 μg/ml) at 4°C overnight, washed three times with TBS-T, and incubated with horseradish peroxidase-conjugated goat anti-rabbit (40 ng/ml; Santa Cruz Biotechnology, Santa Cruz, CA) for 1 h. Identical blots were immunoblotted with preimmune sera for negative controls. The anti-mouse SLC2A1 and SLC2A4 polyclonal antibodies were the generous gift of Dr. Mike Mueckler, Washington University, St. Louis, MO. These antibodies have all been previously characterized as monospecific [25–27]. The anti-mouse SLC2A8 and SLC2A9B polyclonal antibodies were both made by the Moley laboratory and were previously characterized as monospecific [8, 9]. The AKT, phospho (p)-AKT (Ser473), PRKAA (PRKAA), p-PRKAA (p-PRKAA), MAPK3/MAPK1 (MAPK1/2), and p-MAPK3/1 polyclonal antibodies were all obtained from Cell Signaling (Danvers, MA). After washing, the signals were visualized using ECL Western blotting detection reagents (Amersham, Paisley, UK) or SuperSignal West Dura Extended Duration Substrate (Thermo Scientific, Rockford, IL).

Immunofluorescence

Frozen sections (10 μm) were fixed in 3% paraformaldehyde in PBS for 15 min and were washed two times. After blocking with 8% bovine serum albumin (BSA) containing PBS for 1 h, the sections were incubated with the primary antibody (10 μg/ml) at 4°C overnight, washed three times for 5 min with PBS, and incubated with Alexa Fluor 488 goat anti-rabbit (10 μg/ml; Molecular Probes, Eugene, OR) for 30 min. Nuclei were stained with TO-PRO-3 iodide dye (Molecular Probes) by incubating them in 4 mM dye for 20 min. After washing three times in PBS, fluorescence was observed under a confocal microscope using Nikon EZ 7.1 software (Nikon Eclipse E800; Nikon Instruments Corp., Melville, NY). Negative control slides were immunolabeled with preimmune sera. All experiments were performed in triplicate.

Immunohistochemistry

Frozen sections (10 μm) were fixed in 3% paraformaldehyde in PBS for 15 min and were washed two times. After blocking of the endogenous peroxidase activity with 3% H$_2$O$_2$ in methanol for 10 min and blocking of background with 10% nonimmune goat serum for 1 h, the sections were incubated with the primary antibody (10 μg/ml) at 4°C overnight, washed three times for 5 min with PBS, and incubated with biotinylated secondary antibody (Zymed, San Francisco, CA) for 30 min and with enzyme conjugate (streptavidin peroxidase; Zymed) for 30 min. Coloring reaction was performed using 3,3′-diaminobenzidene, and sections were counterstained with hematoxylin (Zymed). All experiments were completed three times.

Injection of Steroid Hormones

To determine the effects of progesterone and estrogen on uterine SLC2A expression, female mice were ovariectomized (OVX) and then rested for 20 days to eliminate circulating ovarian steroids. All steroids were dissolved in sesame oil (Sigma). OVX mice received a single injection of estradiol-17β (E$_2$) (100 ng/mouse), progesterone (P$_4$) (2 mg/mouse), or a combination of the same doses of P$_4$ plus E$_2$. To inhibit E$_2$ receptor action, the anti-E$_2$ Fulvestrant (ICI 182,780; Sigma, 0.5 mg/mouse) was injected 60 min before an injection of E$_2$. This compound not only inhibits transcriptional activity of E$_2$ receptor α but also induces its proteasome-dependent degradation. Control animals were injected with sesame oil vehicle (0.1 ml/mouse). Whole uteri were removed at 1, 6, 12, or 24 h after hormone injection, freed from adjacent fat and mesentery, sliced into small pieces, immediately frozen in cold Friendly Freeze'it (Curtin Matheson Scientific), and stored at −75°C until processed for protein extraction. All experiments were completed three times.

Delayed or Activated Implantation

To induce conditions of delayed implantation, mice were OVX on the morning of Day 4 of pregnancy that was maintained with daily injections of P$_4$ (2 mg/mouse) from Day 5 to Day 7. To terminate delayed implantation and to induce blastocyst activation, a single subcutaneous injection of E$_2$ (25 ng/mouse) was given at the same time as the P$_4$ injection on Day 7. Whole uteri were collected from each group 12 h after the last injection of steroids. Delayed or activated implantation was confirmed by flushed dormant or activated blastocyst. All experiments were performed in triplicate.

Artificial Decidualization

Induction of artificial decidualization was performed as described elsewhere [28]. In brief, OVX mice were allowed 20 days of recovery and were then injected subcutaneously with E$_2$ (100 ng/mouse) for 3 days. After 2 days' rest, E$_2$ (10 ng/mouse) and P$_4$ (1 mg/mouse) were injected subcutaneously for 3 days. At the third day of P$_4$ plus E$_2$ injection, 20 μl of oil was infused intraluminally into the one uterine horn via minilaparotomy, and the other side horn was used as a control. After P$_4$ (1 mg/mouse) injection for 4 days, uteri were collected and frozen. These experiments were performed three times.

Statistical Analysis

Quantification of protein by Western immunoblotting for each group was normalized to β-actin on each gel and was then compared between multiple groups using ANOVA with Fisher exact post hoc test. Significance was defined as $P < 0.05$. Error bars in the figures represent SEMs.

RESULTS

Expression of GLUTs and p-AKT/p-MAPK/p-PRKAA in the Uterus During Estrous Cycles

To determine the expression of GLUTs and the phosphorylation of AKT/MAPK/PRKAA in the mouse uterus during estrous cycles, Western blot and immunofluorescence staining were performed. Expression of the majority of GLUTs (SLC2As 1, 4, 8, and 9B) was highest in the uterus of estrous stage, which is an E$_2$-dominant stage. As shown previously, most SLC2A proteins appear as multiple bands, consistent with their highly glycosylated structures [27]. In metestrous and diestrous stages, which are P$_4$-dominant stages, expression of SLC2As 1, 4, 8, and 9B was lower than that in proestrous stage (Fig. 1A). This difference was significantly lower with GLUT8 and GLUT9B, suggesting hormonal cycle-specific regulation of GLUT expression. Although total AKT did not change between stages, the amount of phosphorylated AKT increased significantly in estrous and metestrous stages and then decreased in diestrous and proestrous stages. The expression pattern of p-GSK3β, which is downstream of AKT, was similar to that of p-AKT (Fig. 1B). Although total MAPK3/MAPK1 and MAPK1/MAPK2 did not change, the phosphorylation of MAPK/MAPK1 was significantly increased in metestrous stage, whereas the phosphorylation of MAPK/MAPK2 was significantly increased in diestrous stage. Both phosphorylated forms were lowest in proestrous stage (Fig. 1C). Total PRKAA/PRKAA fluctuated throughout the cycle, rendering interpretation of the phosphorylation data more difficult (Fig. 1D).

For Figure 1A, three different experiments were performed with three different sets of animals analyzing the four

FIG. 1. Western blot analysis of GLUTs (**A**), AKT/p-AKT (**B**), MAPK/p-MAPK (**C**), and PRKAA/p-PRKAA (**D**) in the mouse uterus during estrous cycles. β-actin was used as an internal control for each set of experiments, and all values are normalized to this and then normalized to proestrous. All facilitative glucose transporters sometimes appear as multiple bands or smears because of different glycosylation states. GLUT1 (SLC2A1) is a doublet at 54–55 kDa. GLUT4 (SLC2A4) is a smear at 55–60 kDa. GLUT8 (SLC2A8) appears as a doublet at 69–72 kDa. GLUT9B (SLC2A9B) is a doublet at 60–61 kDa. These experiments were performed on three separate occasions with different mice. The y-axes represent relative density. $*P < 0.01$ and $**P < 0.001$ compared with proestrous. P, proestrous stage; E, estrous stage; M, metestrous stage; D, diestrous stage.
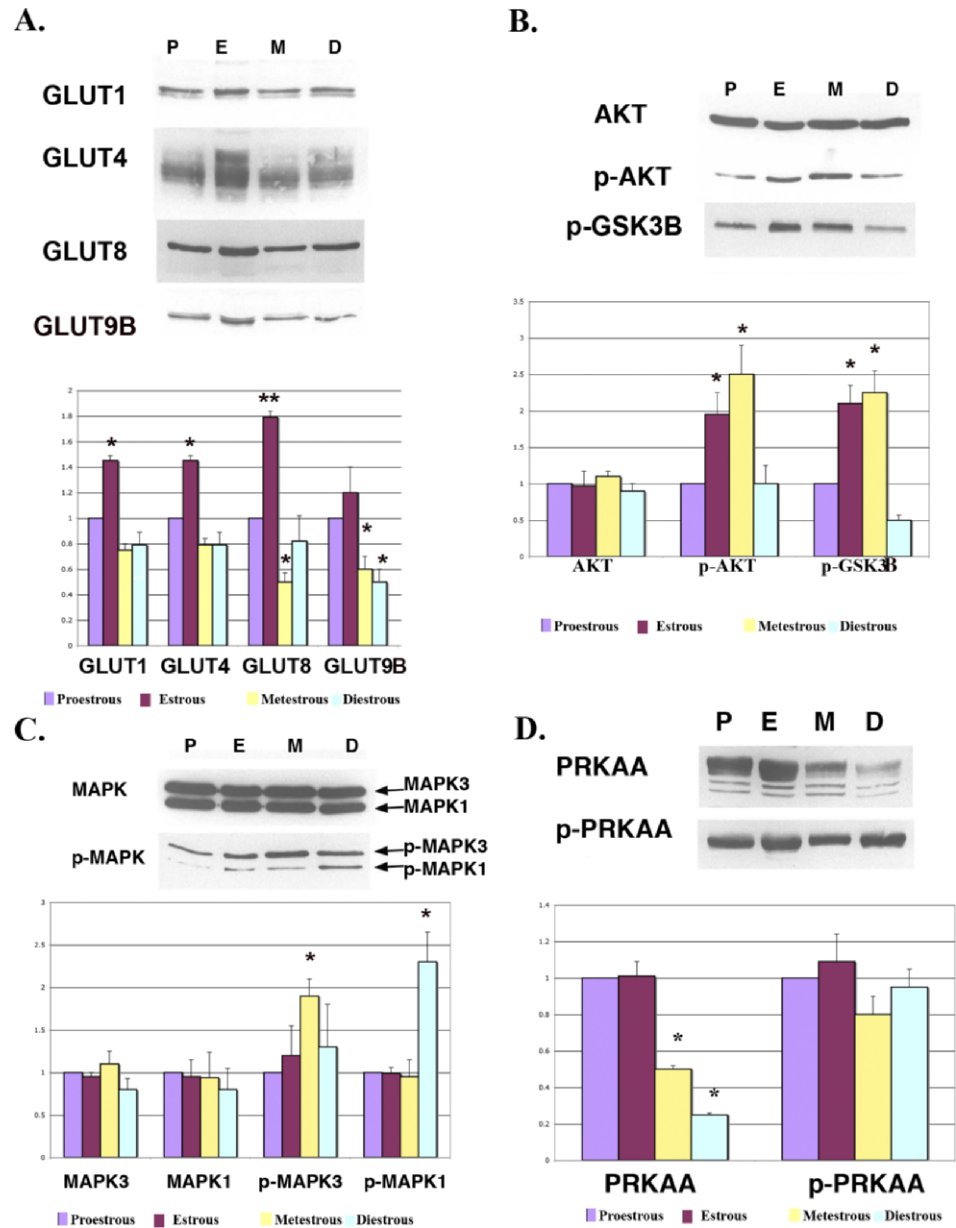
transporters and four different time points. For each experiment, all samples for each transporter were normalized to the proestrous protein level after normalization to actin. All values were then evaluated by one-to-one comparison; thus, there was only 1 *df*. The samples marked with an asterisk represent differences between that group vs. proestrous expression. For B and C in Figure 1, three different experiments were performed with three different sets of animals looking at kinase and the phosphokinase. For each experiment, all samples for each kinase were normalized to the proestrous protein level. Because the kinase levels did not vary significantly among the four points in the estrous cycle, we evaluated by one-to-one comparison the differences between the phosphokinase levels after normalization to proestrous levels. For Figure 1D, we used the same approach; however, PRKAA levels varied, whereas phospho-PRKAA levels did not.

As shown in Figure 2, most SLC2As 1, 8, and 9B proteins in the uterus were localized in the luminal and glandular epithelia. In estrous stage, SLC2As 1, 8, and 9B proteins were highly concentrated in the luminal epithelial surface. At estrous phase, SLC2A1 and SLC2A9B appeared to be exclusively located on the basolateral surfaces of the epithelium, whereas SLC2A8 was located at both the basolateral and apical surfaces of the luminal glandular epithelium. In metestrous and diestrous stages, expression of SLC2As 1, 8, and 9B proteins was decreased. These cyclical changes seen in the epithelium were consistent with the whole-uterine Western analysis shown in Figure 1, supporting the suggestion that the majority of SLC2A protein in the uterus resides at the epithelial surfaces. Stromal expression of SLC2As 1, 8, and 9B was seen but was significantly less than that at the epithelial labeling and was greatest during metestrous and diestrous stages.

Hormonal Regulation of GLUTs Expression in OVX Mice

To determine the factors regulating these changes in GLUT expression and those mediating phosphorylation of kinases, an OVX mouse model was used. Because E_2 and P_4 are essential hormones for the establishment of mouse pregnancy, immunofluorescence for GLUTs was performed to determine whether GLUTs are regulated by these steroid hormones in a
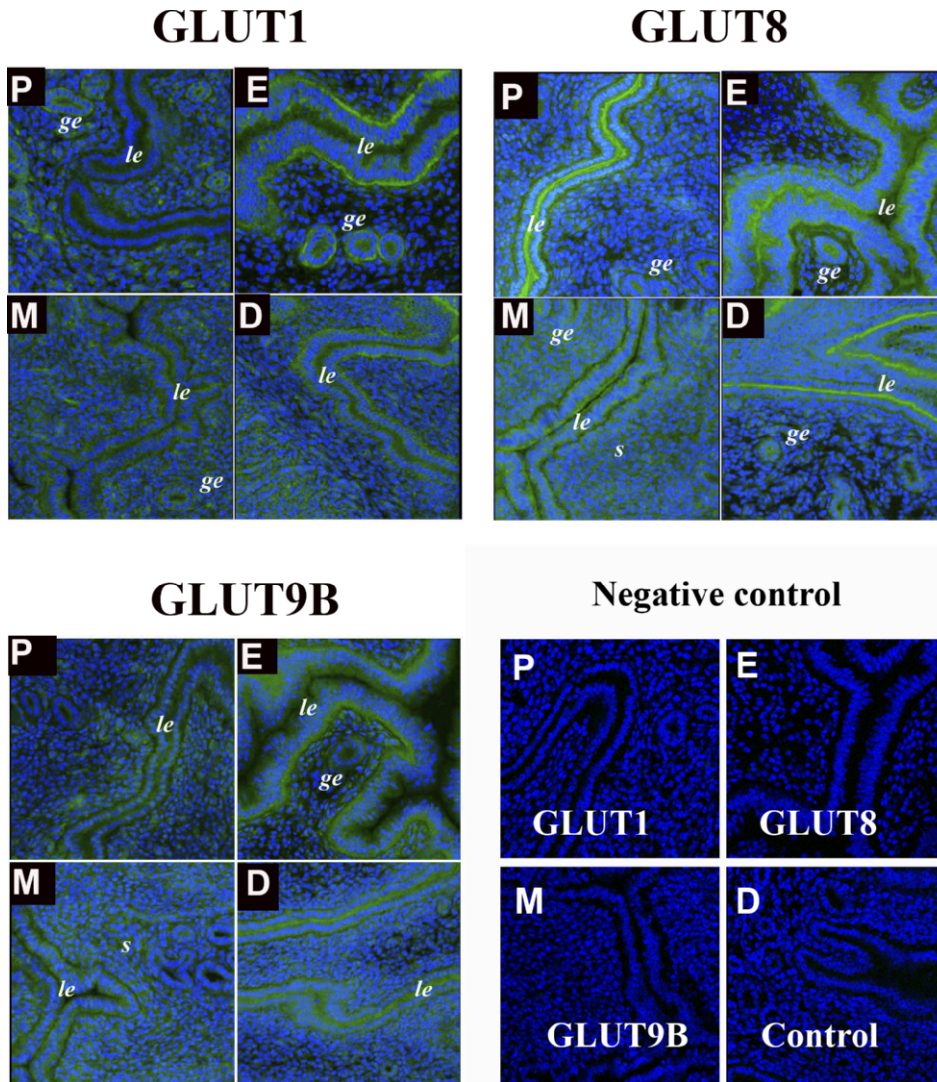
GLUT1

GLUT8

GLUT9B

Negative control

hormone-free OVX mouse model. E_2 treatment resulted in decreased expression of SLC2As 1, 8, and 9B in the luminal epithelial cells. This suppressive effect by E_2 was rescued by injection of the E_2 receptor α antagonist ICI 182,780. Conversely, P_4 treatment caused increased expression of GLUTs in the luminal epithelial cells, and P_4 plus E_2 injection slightly reduced GLUTs expression compared with P_4-only injection (Fig. 3). In addition, cell trafficking of the GLUTs seemed to be altered by this OVX model. Specifically, SLC2A9B appears to be predominantly localized in an intracellular compartment instead of at the cell surface in OXV vs. control murine uterine epithelium. Overall, stromal expression of the GLUTs was much lower in the OVX model compared with cycling mice.

Expression of GLUTs and Cell Signaling Proteins in the Uterus During Peri-Implantation Periods

The subsequent studies focused on the regulation of GLUT expression in vivo during the period of implantation and early pregnancy. IS expression was compared with inter-IS expression in pregnant uteri from Day 5 to Day 8. As shown in Figure 4A, the expression of SLC2As 1, 8, and 9B was increased in the IS vs. inter-IS at selective time points. Expression of SLC2A1 in the IS was significantly increased at Days 6, 7, and 8 ($P < 0.01$, $P < 0.001$, and $P < 0.001$, respectively), but no significant difference was seen at Day 5. The expression of SLC2A8 in the IS also was significantly higher than that in the inter-IS at Days 6, 7, and 8 ($P < 0.05$ for all) but not at Day 5. SLC2A9B expression in the IS was significantly higher at Days 6 and 7 ($P < 0.05$ for both) but not at Day 5 or 8. Conversely, SLC2A4 did not vary significantly between the IS and inter-IS at any time point.

Next, SLC2A expression for each transporter in the IS at the four time points in gestation was expressed as fold increases over inter-IS expression, and these time point expression levels were compared among SLC2A groups (Fig. 4B). SLC2A1 expression was significantly higher in IS on Days 7 and 8 compared with either Day 5 or Day 6 (Day 7 vs. Day 5 or 6, $P < 0.01$; Day 8 vs. Day 5 or 6, $P < 0.01$). SLC2A8 expression increased gradually from Day 5 to Day 8 in IS. A significant difference in expression was only seen between Day 5 and Day 8 ($P < 0.01$). SLC2A9B expression increased slightly in IS; however, a significant difference was only seen between Day 5 and Day 8. Finally, SLC2A4 did not change in expression significantly over the time points in gestation.

To localize the SLC2As in the pregnant uterus, immunohistochemistry was performed. SLC2As 1, 8, and 9B were differently localized between IS and inter-IS. In inter-IS, they were concentrated in the luminal and glandular epithelial cells but not in stromal cells. In IS, they were mainly localized in the
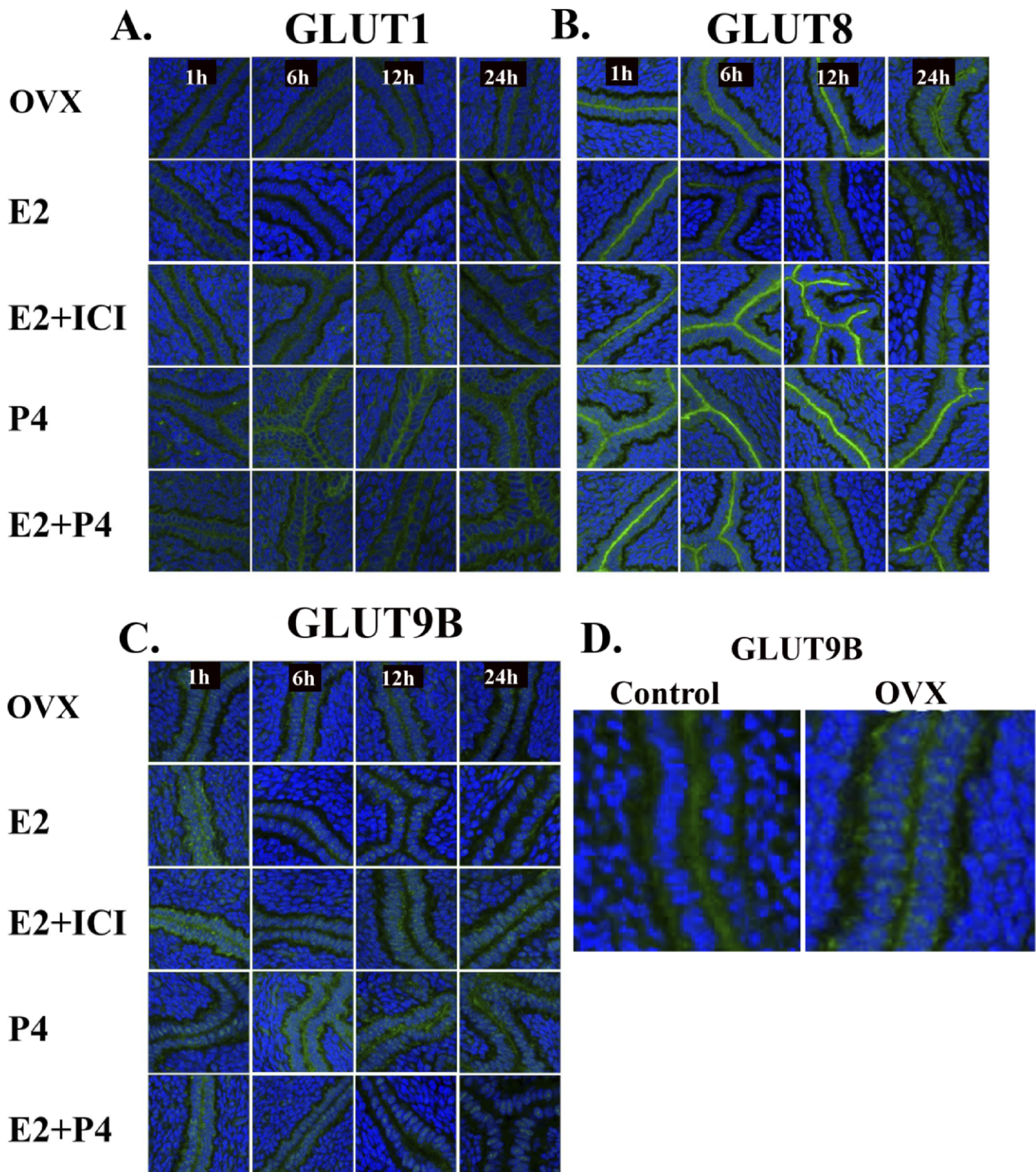
FIG. 3.   Immunofluorescence of GLUTs in the OVX mouse uterus. Paraformaldehyde-fixed tissue slices were incubated with primary antibodies to SLC2A1 (GLUT1) (**A**), SLC2A8 (GLUT8) (**B**), or SLC2A9B (GLUT9B) (**C**). Slides were then incubated with a secondary antibody, Alexa Fluor 488 goat anti-rabbit IgG (green fluorescence). To-Pro-3 iodide was used to stain the nuclei (blue fluorescence). ICI 182,780 was injected 1 h before E_2 injection, and specimens were obtained at 1, 6, 12, and 24 h after E_2 injection. E2, estrogen injection; P4, progesterone injection. This experiment was performed on five separate occasions with different mice. **D**) Higher magnification of uterine epithelial protein expression of GLUT9B (SLC2A9B) in control cycling mice vs. OVX mice without hormone supplementation. Original magnification ×20 (**A–C**) and ×40 (**D**).
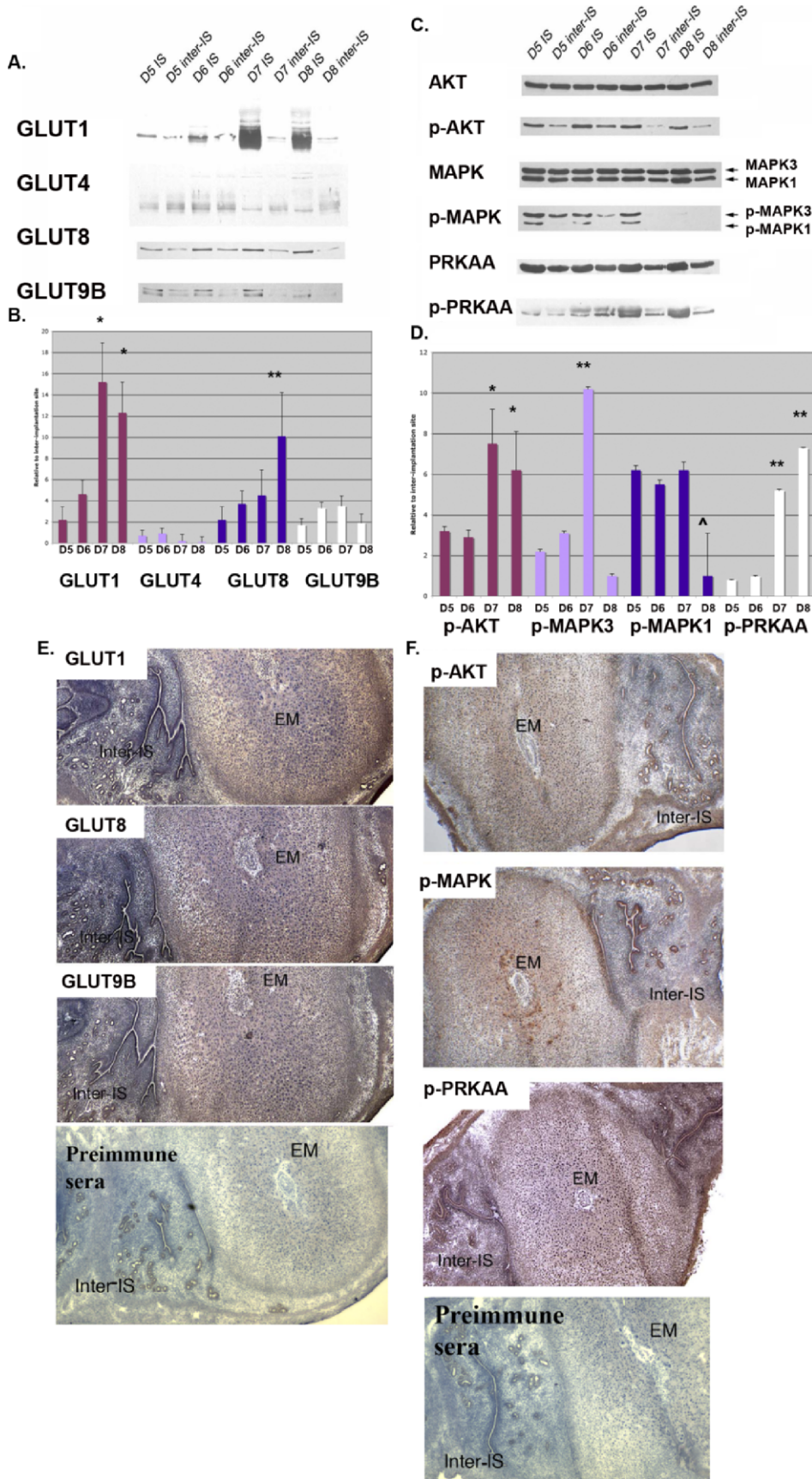
FIG. 4. Protein expression in mouse uteri during the peri-implantation period. Western blot analysis of GLUTs (**A**) and p-AKT, p-MAPK, and p-PRKAA (**C**) in IS and inter-IS. β-actin was used as an internal control for each individual gel, and IS vs. inter-IS expression is compared at each day. For the kinase, phosphorylated forms were normalized to total kinase. **B** and **D**) Next, protein quantification was expressed as fold increase of IS over inter-IS expression, and comparisons were made among each SLC2A or kinase group. **B**) *$P < 0.01$ for SLC2A Day 5 or 6 vs. Day 7 or 8 and **$P < 0.01$ for Day 5 vs. Day 8 only. **D**) *$P < 0.01$ for p-AKT Day 5 or 6 vs. Day 7 or 8, **$P < 0.001$ for p-MAPK3 for Day 7 vs. all other time points, ^$P < 0.05$ for p-MAPK1 for Day 8 vs. all other time points, and **$P < 0.001$ for p-PRKAA for Days 7 and 8 vs. Days 5 and 6. Immunohistochemistry of SLC2As (**E**) and p-AKT, p-MAPK, and p-PRKAA (**F**) in the Day 7 mouse uterus was performed on longitudinally sectioned uterus incubated with primary antibodies. Slides were then incubated with biotinylated secondary antibody and with enzyme conjugate. Coloring reaction was performed using 3,3'-diaminobenzidene, and sections were counterstained with hematoxylin. EM, embryo. This experiment was performed on four separate occasions with different mice. Original magnification ×20.
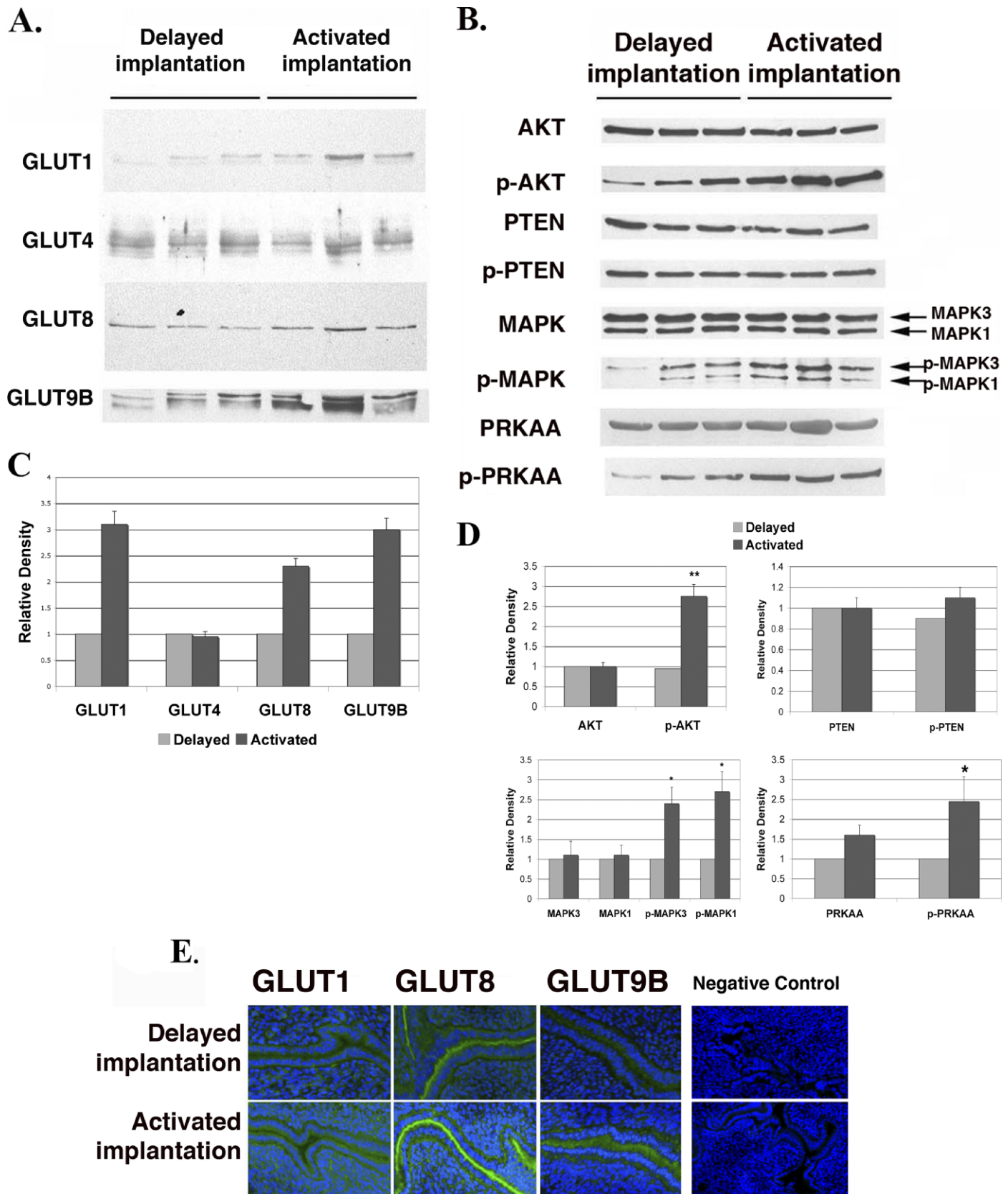
FIG. 5. Protein expression of GLUTs and signaling pathway kinases in uteri of the delayed and activated implantation models. Western blot analysis of GLUTs (**A**) and p-AKT, p-MAPK, and p-PRKAA (**B**). Three lanes per group are shown. β-actin was used as an internal control, and the quantitative data are shown in (**C**) and (**D**). Each individual lane was normalized to the corresponding β-actin first and then to the delayed implantation values. The y-axes represent relative density. *$P < 0.01$ and **$P < 0.001$ compared with delayed implantation. **E**) Immunohistochemistry of GLUTs in the mouse uterus of the delayed or activated model using tissue slices incubated with primary antibodies. Slides were then incubated with a secondary antibody, Alexa Fluor 488 goat anti-rabbit IgG (green fluorescence). To-Pro-3 iodide was used to stain the nuclei (blue fluorescence). Negative control preimmune sera for these antibodies are shown in Figure 2. The negative control seen here is immunohistochemistry without a secondary antibody. This experiment was performed on five separate occasions with different mice. Original magnification ×20.

decidual region of the stromal cells (Fig. 4E), suggesting a role for the GLUTs in decidualization.

Next, phosphorylated or activated AKT, MAPK3/1, and PRKAA were normalized to total unphosphorylated protein at each time point, and these values for each time point in gestation (Days 5–8) were compared between IS and inter-IS (Fig. 4C). p-AKT was significantly greater in the IS at all time points ($P < 0.01$ for all) compared with inter-IS. p-MAPK3 was significantly greater at all time points in the IS except Day 8, when it was barely detected in the phosphorylated form ($P < 0.01$ for Days 5 and 6 and $P < 0.001$ for Day 7). p-MAPK1 was similar, with significantly greater IS detected at Days 5–7 ($P < 0.001$), but no significance was seen between IS and inter-IS at Day 8. IS P-PRKAA was significantly higher than inter-IS expression at Days 7 and 8 ($P < 0.001$) but not at Days 5 and 6.

Finally, phosphorylated forms of these signaling kinases in the IS at the four time points in gestation were expressed as fold increases over inter-IS-detected levels, and phosphorylated forms at these time point were compared among each kinase (Fig. 4D). p-AKT was significantly higher at Days 7 and 8 vs. both Days 5 and 6 ($P < 0.01$ for Day 5 vs. Day 7, Day 5 vs. Day 8, Day 6 vs. Day 7, and Day 6 vs. Day 8). p-MAPK3 was significantly higher at Day 7 than at all other time points ($P < 0.001$ for all). p-MAPK1 was not significantly increased between Day 5 and Day 7; however, p-MAPK1 was barely detectable at Day 8 and thus was significantly decreased at this point compared with Days 5–7 ($P < 0.05$). IS p-PRKAA expression at Day 7 and Day 8 was significantly higher than at Day 5 and Day 6 ($P < 0.001$ for Day 5 vs. Day 7, Day 5 vs. Day 8, Day 6 vs. Day 7, and Day 6 vs. Day 8).

By immunohistochemistry, p-AKT, p-MAPK, and p-PRKAA were localized in luminal and glandular epithelial cells of the inter-IS and in the decidual region of the IS, with similar localization patterns of GLUTs. These results are summarized in Figure 4F.

For all data in Figure 4, three different experiments were performed with three different sets of animals analyzing the four different transporters expressed at IS at four different time points. All expression was normalized to its corresponding inter-IS expression level. The fold difference in the level of expression between time points was compared by one-to-one comparison.

Expression of GLUTs in the Uterus of the Delayed or Activated Implantation Model

To determine whether the expression of GLUTs is dependent on the activation of implantation of the blastocyst, we analyzed the levels of expression of GLUTs, p-AKT, p-MAPK3/1, and p-PRKAA in the uterus of the delayed and activated implantation model as described previously [28]. By 12 h after the termination of delayed implantation and the initiation of activated implantation by E$_2$ injection, the expression of SLC2As 1, 8, and 9B was increased (Fig. 5, A and C) in the uterus of the activated implantation model. The expression of p-AKT, p-MAPK3/1, and p-PRKAA was also increased in the uterus of the activated implantation model. p-PTEN, which is a suppressor for p-AKT, was similar between both groups (Fig. 5, B and D). Compared with delayed implantation, increased intensity for GLUTs was seen in the luminal epithelial cells of activated implantation (Fig. 5E), suggesting that either the presence of the blastocyst and/or the injection of E$_2$ increased expression of the GLUTs.

For data presented in Figure 5, three different experiments were performed with three different sets of animals analyzing
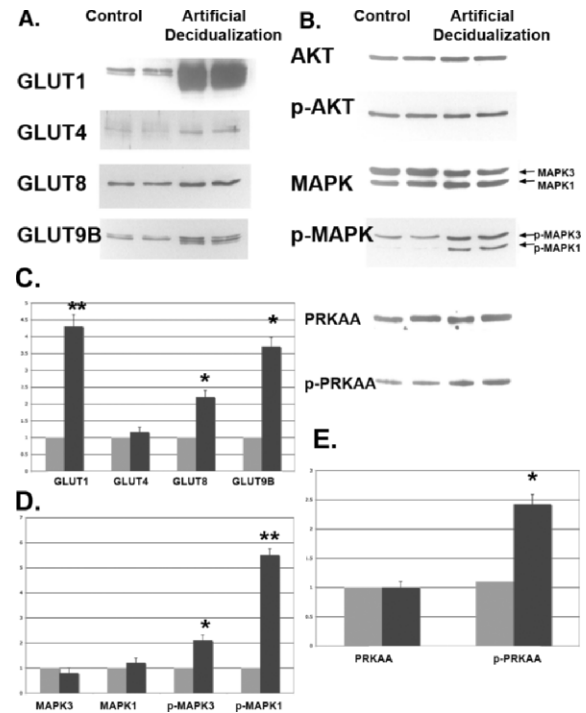

FIG. 6. Western blot analysis of GLUTs (**A**) and p-AKT, p-MAPK, and p-PRKAA (**B**) in the mouse uterus of the artificial decidualization model. The Western immunoblots (**A** and **B**) were quantitated using β-actin as the internal control for each blot and then normalized to control (**C–E**). Two lanes per group are shown. Oil-infused uterine horn was used as the uterus of the artificial decidualization model (black bars), and the other side horn (which is not an oil-infused horn) was used as a control (gray bars). This experiment was performed on six separate occasions with different mice. The y-axes represent relative density. *$P < 0.01$ and **$P < 0.001$ compared with control.

the four transporters under two different conditions. For each experiment, samples for each transporter were normalized to the protein level in the delayed implantation group. All values were then analyzed by one-to-one comparison; thus, there was 1 df. Data points with asterisks represent differences between that group and the delayed implantation group.

Increased GLUTs Expression and MAPK/PRKAA Phosphorylation in the Uterus of the Artificial Decidualization Model

To examine whether GLUTs expression and AKT/MAPK/PRKAA activation in uterine cells are affected by artificial decidualization, we induced decidualization with intrauterine oil injection and hormone replacement following ovariectomy. During normal pregnancy, uterine stromal cells differentiate into decidual cells in response to an activated implanting blastocyst. The decidual response, however, can be induced in the absence of a blastocyst if the uterus is hormonally primed either by pseudopregnancy or by 48 h of P$_4$ injections in an OVX mouse [28]. As shown in Figure 6 (A and C), expression of SLC2As 1, 4, 8, and 9B in uteri of the artificial decidualization model was dramatically higher than that in control uteri. The phosphorylation of MAPK3/1 and PRKAA in uteri of the artificial decidualization model was also higher than that in control uteri (Fig. 6, B, D, and E); however, no change was seen in levels of AKT or p-AKT. For the data in Figure 6, four different experiments were performed with four

different sets of animals analyzing the four transporters under two different conditions.

DISCUSSION

In this study, we have demonstrated that GLUTs and activated AKT/MAPK/PRKAA signaling proteins are expressed and regulated by steroid hormones in the mouse uterus and uterine epithelium during estrous cycles and the peri-implantation periods. Moreover, we have shown using models of artificial decidualization and delayed/activated implantation that glucose utilization has a key role in these processes and in early endometrial differentiation during pregnancy. Recent findings show that only SLC2A1 and SLC2A3 are expressed in human endometrium and are increased at secretory phase and in decidua [29]. Another study [30] shows that SLC2A1 and SLC2A8 are expressed in human endometrium and in endometrial cancer. In addition, SLC2A1, SLC2A3, and SLC2A4 are expressed in the rat uterus and are highly increased in the decidual cells of IS [15, 31]. Previous studies show that SLC2A1 and SLC2A3 mRNA is expressed in the placenta and decidua of the pregnant mouse [32], and mRNA is expressed in nonpregnant mouse uterus [15]. These observations led us to focus on the regulation of GLUT expression in the uterine epithelium of pregnant mice, as well as on the activation of kinases involved in growth factor- and nutrient-triggered pathways in the uterus.

Using cycling mice, as well as murine models of delayed implantation and artificial decidualization, our results demonstrate dramatic changes in the expression of SLC2As 1, 8, and 9B in epithelium during the menstrual cycle and the peri-implantation period and in the uteri of an artificial decidualization model (Figs. 4 and 6). This suggests that mice deficient in SLC2A1 and SLC2A8 expression (the only two null mice described thus far among those GLUTs identified in this work as being hormonally responsive in murine uteri) may have smaller litter sizes due to problems with establishment and maintenance of pregnancy. We observed decreased numbers of pups with the SLC2A1 antisense transgenic mouse [33] and with the SLC2A8 null mouse we have created (Kim and Moley, unpublished results). SLC2A1 appears predominantly to be basolateral, whereas SLC2A8 is apical. SLC2A1 is a well-characterized basolateral transporter [34]; however, SLC2A8 has been reported to be predominantly located in intracellular compartments [35–37] that traffic to the plasma membrane with insulin or IGF-1 in embryonic cells [35] and with PRKAA activation in trophoblast stem cells [38]. It appears that the uterine epithelial SLC2A8 transporters are translocated to the apical surface possibly due to the maximal activation of PRKAA at this same time point (Days 7 and 8 of pregnancy) as shown in Figure 4. This expression pattern parallels AKT and MAPK1 and MAPK 2 phosphorylation; however, both MAPKs decrease their phosphorylation state by Day 8. These findings suggest that the hormonal changes associated with early pregnancy (fluctuations in E_2, P_4, and/or growth factors) lead to alterations in nutrient-dependent signaling pathways (PRKAA, MAPK, and AKT), resulting in changes in GLUT expression. This apical-specific localization of the high-affinity SLC2A8 (Km, 2 mM) may serve to maximize glucose utilization from the luminal surface to support implantation. SLC2A1, a lower-affinity transporter with a Michaelis-Menton constant (Km) of 6–8 mM, is present on the basolateral surface, presumably to facilitate transport of glucose into the stromal compartment. In this study, the expression of this transporter increases in the basolateral compartment simultaneously with

SLC2A8, supporting our hypothesis that the hormonal and metabolic changes are synchronized.

To test this hypothesis, we next performed whole-animal ovariectomy and delayed implantation studies, as well as artificial decidualization assays. SLC2A8 localization at the apical epithelial surface was consistently seen in all groups; however, in vivo P_4 treatment in all models with or without E_2 appeared to increase expression of this transporter. SLC2A1 expression was seen at the basolateral surfaces in both models, and P_4 plus E_2 appeared to lead to the greatest level of expression. It is unclear if any of these manipulated systems mimic the in vivo pregnancy state in the epithelium; however, we can conclude that the hormonal changes associated with pregnancy affect GLUT expression.

Surprisingly, we discovered that SLC2A9B was localized at the basolateral surfaces of the endometrial epithelium, whereas we had previously identified SLC2A9B at the apical surfaces of polarized cells [39]. Moreover, we found that localization of SLC2A9B in the uterine epithelium varied between control cycling mice and OVX mice (Fig. 3D). This finding suggests that trafficking of this GLUT may be dependent on circulating or local hormone levels. GLUT9 localization has previously been found to vary in embryo development, with cell surface localization in cleavage-stage embryos and relocalization to an intracellular compartments on blastocyst formation [13]. This hormonally regulated localization of SLC2A9, which appears to differ from the other two transporters, may be related to the more varied substrate specific to SLC2A9. We have previously reported that this transporter is a high-affinity transporter for glucose (Km, 0.6 mM) and fructose (Km, 0.4 mM) but does not transport galactose [40]. In addition, we have recently published our findings showing that SLC2A9 is a high-capacity urate transporter (Km, 300 μM) [41]. For these reasons, it is possible that the different localization of this transporter may be due to changes in substrate preference during the process of preparation for implantation. Future studies will be needed to test this hypothesis. These results with all the SLC2A proteins lead us to conclude that epithelial glucose utilization, as well as possibly other substrates through the facilitative GLUTs, is highly regulated in the uterus and has an important role in establishing adequate implantation. It is possible that abnormalities in this process may be responsible in part for high rates of recurrent failed pregnancies in some populations of women.

These studies also demonstrate significant changes in AKT/MAPK/PRKAA signaling in endometrial tissue in response to hormonal changes. As a major component of the PI3-kinase signaling pathway, AKT in response to insulin controls glucose uptake by regulating insulin-mediated SLC2A4 translocation [17]. In addition, p-AKT is increased in human decidual cells [42, 43] and prevents apoptosis, while promoting differentiation in the hormonally responsive mammary epithelium [44]. Recent studies demonstrate that activated AKT and MAPK3/1 regulate trophoblast invasion via chorionic gonadotropin [45] and that prolactin induces MAPK phosphorylation in the glandular epithelium and the CD56$^+$ natural killer cells within the stromal compartment of the human endometrium [18]. AMP-activated protein kinase (PRKAA) is activated by increase of the AMP:ATP ratio [20]. PRKAA has a key role in energy metabolism (e.g., fatty acid oxidation and synthesis, glucose uptake, and cholesterol synthesis [21, 22]). In addition, SLC2A4 translocation is mediated by PRKAA signaling in heart and skeletal muscle [23, 24]. AKT/MAPK/PRKAA signaling has not been described in mouse uterus during the peri-implantation period, to our knowledge. We believe that this study shows for the first time that the phosphorylation of

AKT/MAPK/PRKAA is regulated by E_2 and P_4 in the delayed implantation and artificial decidualization models and occurs in pregnant uteri. Phosphorylation of AKT/MAPK/PRKAA was dramatically increased in the decidual region of the IS (Fig. 4, C, D, and F) and was significantly increased in the uterus of the activated implantation model (Fig. 5, B, D, and E). Moreover, expression levels of p-MAPK and p-PRKAA in uteri of the artificial decidualization model were dramatically higher than those in control uteri (Fig. 6B). The different pattern of p-AKT expression between IS (Fig. 4B) and that in the artificial decidualization model of the uterus (Fig. 6B) could be explained by IGF signaling from the embryo. Reduced p-AKT signaling may be compensated for by MAPK/PRKAA in an artificial decidualization model. This suggests that AKT/MAPK/PRKAA signaling may have an important role in the decidualization process.

In conclusion, the results of this study suggest that glucose utilization through uterine epithelial GLUTs and AKT/MAPK/PRKAA signaling pathways is regulated by steroid hormones in the mouse uterus and may have important roles in preparation for implantation, decidualization of murine uterine cells, and maintenance of pregnancy. Therefore, maternal abnormalities in glucose metabolism or decreased E_2/P_4 signaling may manifest as implantation failures and poor pregnancy outcomes.

REFERENCES

1. Joost HG, Bell GI, Best JD, Birnbaum MJ, Charron MJ, Chen YT, Doege H, James DE, Lodish HF, Moley KH, Moley JF, Mueckler M, et al. Nomenclature of the GLUT/SLC2A family of sugar/polyol transport facilitators. Am J Physiol Endocrinol Metab 2002; 282:E974–E976.
2. Joost HG, Thorens B. The extended GLUT-family of sugar/polyol transport facilitators: nomenclature, sequence characteristics, and potential function of its novel members (review). Mol Membr Biol 2001; 18:247–256.
3. Wood IS, Trayhurn P. Glucose transporters (GLUT and SGLT): expanded families of sugar transport proteins. Br J Nutr 2003; 89:3–9.
4. Riley JK, Moley KH. Glucose utilization and the PI3-K pathway: mechanisms for cell survival in preimplantation embryos. Reproduction 2006; 131:823–835.
5. Mueckler M. Family of glucose-transporter genes: implications for glucose homeostasis and diabetes. Diabetes 1990; 39:6–11.
6. Fukumoto H, Kayano T, Buse JB, Edwards Y, Pilch PF, Bell GI, Seino S. Cloning and characterization of the major insulin-responsive glucose transporter expressed in human skeletal muscle and other insulin-responsive tissues. J Biol Chem 1989; 264:7776–7779.
7. Birnbaum MJ. Identification of a novel gene encoding an insulin-responsive glucose transporter protein. Cell 1989; 57:305–315.
8. Carayannopoulos MO, Chi MM, Cui Y, Pingsterhaus JM, McKnight RA, Mueckler M, Devaskar SU, Moley KH. GLUT8 is a glucose transporter responsible for insulin-stimulated glucose uptake in the blastocyst. Proc Natl Acad Sci U S A 2000; 97:7313–7318.
9. Kim ST, Moley KH. The expression of GLUT8, GLUT9a, and GLUT9b in the mouse testis and sperm. Reprod Sci 2007; 14:445–455.
10. Gomez O, Romero A, Terrado J, Mesonero JE. Differential expression of glucose transporter GLUT8 during mouse spermatogenesis. Reproduction 2006; 131:63–70.
11. Doege H, Schurmann A, Bahrenberg G, Brauers A, Joost HG. GLUT8, a novel member of the sugar transport facilitator family with glucose transport activity. J Biol Chem 2000; 275:16275–16280.
12. Kim ST, Moley K. Paternal effect on embryo quality in diabetic mice is related to poor sperm quality and associated with decreased GLUT expression. Reproduction 2008; 136:313–322.
13. Carayannopoulos MO, Schlein A, Wyman A, Chi M, Keembiyehetty C, Moley KH. GLUT9 is differentially expressed and targeted in the preimplantation embryo. Endocrinology 2004; 145:1435–1443.
14. Keembiyehetty C, Augustin R, Carayannopoulos MO, Steer S, Manolescu A, Cheeseman CI, Moley KH. Mouse glucose transporter 9 splice variants are expressed in adult liver and kidney and are up-regulated in diabetes. Mol Endocrinol 2006; 20:686–697.
15. Zhou J, Bondy CA. Placental glucose transporter gene expression and metabolism in the rat. J Clin Invest 1993; 91:845–852.
16. Bryant NJ, Govers R, James DE. Regulated transport of the glucose transporter GLUT4. Nat Rev Mol Cell Biol 2002; 3:267–277.
17. Pessin JE, Saltiel AR. Signaling pathways in insulin action: molecular targets of insulin resistance. J Clin Invest 2000; 106:165–169.
18. Gubbay O, Critchley HO, Bowen JM, King A, Jabbour HN. Prolactin induces ERK phosphorylation in epithelial and CD56(+) natural killer cells of the human endometrium. J Clin Endocrinol Metab 2002; 87:2329–2335.
19. Klotz DM, Hewitt SC, Ciana P, Raviscioni M, Lindzey JK, Foley J, Maggi A, DiAugustine RP, Korach KS. Requirement of estrogen receptor-alpha in insulin-like growth factor-1 (IGF-1)-induced uterine responses and in vivo evidence for IGF-1/estrogen receptor cross-talk. J Biol Chem 2002; 277:8531–8537.
20. Corton JM, Gillespie JG, Hardie DG. Role of the AMP-activated protein kinase in the cellular stress response. Curr Biol 1994; 4:315–324.
21. Kemp BE, Mitchelhill KI, Stapleton D, Michell BJ, Chen ZP, Witters LA. Dealing with energy demand: the AMP-activated protein kinase. Trends Biochem Sci 1999; 24:22–25.
22. Hardie DG, Scott JW, Pan DA, Hudson ER. Management of cellular energy by the AMP-activated protein kinase system. FEBS Lett 2003; 546:113–120.
23. Russell RR III, Bergeron R, Shulman GI, Young LH. Translocation of myocardial GLUT-4 and increased glucose uptake through activation of AMPK by AICAR. Am J Physiol 1999; 277:H643–H649.
24. Li J, Hu X, Selvakumar P, Russell RR III, Cushman SW, Holman GD, Young LH. Role of the nitric oxide pathway in AMPK-mediated glucose uptake and GLUT4 translocation in heart muscle. Am J Physiol Endocrinol Metab 2004; 287:E834–E841.
25. Marshall BA, Murata H, Hresko RC, Mueckler M. Domains that confer intracellular sequestration of the Glut4 glucose transporter in Xenopus oocytes. J Biol Chem 1993; 268:26193–26199.
26. Marshall BA, Ren JM, Johnson DW, Gibbs EM, Lillquist JS, Soeller WC, Holloszy JO, Mueckler M. Germline manipulation of glucose homeostasis via alteration of glucose transporter levels in skeletal muscle. J Biol Chem 1993; 268:18442–18445.
27. Tordjman KM, Leingang KA, James DE, Mueckler MM. Differential regulation of two distinct glucose transporter species expressed in 3T3-L1 adipocytes: effect of chronic insulin and tolbutamide treatment. Proc Natl Acad Sci U S A 1989; 86:7761–7765.
28. Deb K, Reese J, Paria BC. Methodologies to study implantation in mice. Methods Mol Med 2006; 121:9–34.
29. von Wolff M, Ursel S, Hahn U, Steldinger R, Strowitzki T. Glucose transporter proteins (GLUT) in human endometrium: expression, regulation, and function throughout the menstrual cycle and in early pregnancy. J Clin Endocrinol Metab 2003; 88:3885–3892.
30. Goldman NA, Katz EB, Glenn AS, Weldon RH, Jones JG, Lynch U, Fezzari MJ, Runowicz CD, Goldberg GL, Charron MJ. GLUT1 and GLUT8 in endometrium and endometrial adenocarcinoma. Mod Pathol 2006; 19:1429–1436.
31. Korgun ET, Demir R, Hammer A, Dohr G, Desoye G, Skofitsch G, Hahn T. Glucose transporter expression in rat embryo and uterus during decidualization, implantation, and early postimplantation. Biol Reprod 2001; 65:1364–1370.
32. Yamaguchi M, Sakata M, Ogura K, Miyake A. Gestational changes of glucose transporter gene expression in the mouse placenta and decidua. J Endocrinol Invest 1996; 19:567–569.
33. Heilig CW, Saunders T, Brosius FC III, Moley K, Heilig K, Baggs R, Guo L, Conner D. Glucose transporter-1-deficient mice exhibit impaired development and deformities that are similar to diabetic embryopathy. Proc Natl Acad Sci U S A 2003; 100:15613–15618.
34. Pascoe WS, Inukai K, Oka Y, Slot JW, James DE. Differential targeting of facilitative glucose transporters in polarized epithelial cells. Am J Physiol 1996; 271:C547–C554.
35. Carayannopoulos M, Chi M, Cui Y, Pingsterhaus J, Moley K. GLUT8, a glucose transporter responsible for insulin-stimulated uptake in the blastocyst. Proc Natl Acad Sci U S A 2000; 97:7313–7318.
36. Augustin R, Riley J, Moley KH. GLUT8 contains a [DE]XXXL[LI] sorting motif and localizes to a late endosomal/lysosomal compartment. Traffic 2005; 6:1196–1212.
37. Wyman AH, Chi M, Riley J, Carayannopoulos MO, Yang C, Coker KJ, Pessin JE, Moley KH. Syntaxin 4 expression affects glucose transporter 8 translocation and embryo survival. Mol Endocrinol 2003; 17:2096–2102.
38. Louden E, Chi M, Moley K. Crosstalk between the AMP-activated kinase

and insulin signaling pathways rescues murine blastocyst cells from insulin resistance. Reproduction 2008; 136:335–344.

39. Augustin R, Carayannopoulos MO, Dowd LO, Phay JE, Moley JF, Moley KH. Identification and characterization of human glucose transporter-like protein-9 (GLUT9): alternative splicing alters trafficking. J Biol Chem 2004; 279:16229–16236.

40. Manolescu A, Augustin R, Moley KH, Cheeseman CI. A highly conserved hydrophobic motif in the exofacial vestibule of fructose transporting SLC2A proteins acts as a critical determinant of their substrate selectivity. Mol Membr Biol 2007; 24:455–463.

41. Caulfield MJ, Munroe PB, O'Neill D, Witkowska K, Charchar FJ, Doblado M, Evans S, Eyheramendy S, Onipinla A, Howard P, Shaw-Hawkins S, Dobson RJ, et al. SLC2A9 is a high-capacity urate transporter in humans. PLoS Med 2008; 5:e197.

42. Yoshino O, Osuga Y, Hirota Y, Koga K, Yano T, Tsutsumi O, Taketani Y. Akt as a possible intracellular mediator for decidualization in human endometrial stromal cells. Mol Hum Reprod 2003; 9:265–269.

43. Toyofuku A, Hara T, Taguchi T, Katsura Y, Ohama K, Kudo Y. Cyclic and characteristic expression of phosphorylated Akt in human endometrium and decidual cells in vivo and in vitro. Hum Reprod 2006; 21:1122–1128.

44. Maroulakou IG, Oemler W, Naber SP, Klebba I, Kuperwasser C, Tsichlis PN. Distinct roles of the three Akt isoforms in lactogenic differentiation and involution. J Cell Physiol 2008; 217:468–477.

45. Prast J, Saleh L, Husslein H, Sonderegger S, Helmer H, Knofler M. Human chorionic gonadotropin stimulates trophoblast invasion through extracellularly regulated kinase and AKT signaling. Endocrinology 2008; 149:979–987.